

A microscopic refrigeration process triggered through spin-crossover mechanism

P. J. von Ranke

Citation: *Appl. Phys. Lett.* **110**, 181909 (2017); doi: 10.1063/1.4982792

View online: <http://dx.doi.org/10.1063/1.4982792>

View Table of Contents: <http://aip.scitation.org/toc/apl/110/18>

Published by the [American Institute of Physics](#)

Articles you may be interested in

[¹¹⁹Sn Mössbauer spectroscopy for assessing the local stress and defect state towards the tuning of Ni-Mn-Sn alloys](#)

Appl. Phys. Lett. **110**, 181908181908 (2017); 10.1063/1.4982630

[Polarization map of correlated sideband generation in vectorial four-wave mixing](#)

Appl. Phys. Lett. **110**, 181108181108 (2017); 10.1063/1.4982209

[Tuning electrical conductivity, charge transport, and ferroelectricity in epitaxial BaTiO₃ films by Nb-doping](#)

Appl. Phys. Lett. **110**, 182903182903 (2017); 10.1063/1.4982655

[Phase inversion of slug flow on step surface to form high viscosity droplets in microchannel](#)

Appl. Phys. Lett. **110**, 181601181601 (2017); 10.1063/1.4982632

[Band alignment of lateral two-dimensional heterostructures with a transverse dipole](#)

Appl. Phys. Lett. **110**, 181602181602 (2017); 10.1063/1.4982791

[Microwave metamaterials made by fused deposition 3D printing of a highly conductive copper-based filament](#)

Appl. Phys. Lett. **110**, 181903181903 (2017); 10.1063/1.4982718

Fearful for the future of science?

Sign up for FREE FYI emails.
AIP American Institute of Physics

A microscopic refrigeration process triggered through spin-crossover mechanism

P. J. von Ranke^{a)}

Dep. de Eletrônica Quântica, Instituto de Física, Universidade do Estado do Rio de Janeiro UERJ, Rua São Francisco Xavier, 524, 20550-013 Rio de Janeiro, RJ, Brazil

(Received 15 March 2017; accepted 19 April 2017; published online 2 May 2017)

We report the giant barocaloric effect determined in a spin-crossover system using a microscopic model. Compared with the widely used gas compression-expansion refrigeration technology, field induced refrigeration in solid materials reduces environmental damages and improves the energy efficiency. The origin of the giant effect was ascribed to the entropic phonon contribution arising from low spin to high spin phase transition, induced by a pressure change. Here, we show that for the applied pressure variation from 1 bar to 4.1 kbar, the isothermal entropy change (ΔS_T) in a one-dimensional spin crossover system $[\text{Fe}(\text{hyptrz})_3](4\text{-chlorophenylsulfonate})_2\text{H}_2\text{O}$ achieves a maximum value of $55.8 \text{ J mol}^{-1} \text{ K}^{-1}$ at 191 K, leading to a huge refrigerant capacity of 2160 J mol^{-1} . Our results were compared with the results of other giant solid refrigerant materials such as $(\text{NH}_4)_2\text{SO}_4$, $\text{Gd}_5\text{Si}_2\text{Ge}_2$, and $\text{Gd}_5[\text{Si}_{0.43}\text{Ge}_{0.57}]_4$. *Published by AIP Publishing.*
[\[http://dx.doi.org/10.1063/1.4982792\]](http://dx.doi.org/10.1063/1.4982792)

The potential of a solid refrigerant material is characterized by the isothermal entropy change ΔS_T upon controlled external field variations. If ΔS_T is obtained upon magnetic field variations, a magnetocaloric effect occurs; upon an electrical field change or a pressure change, electrocaloric or barocaloric effects occur, respectively.¹ Refrigerators based on solid refrigerant materials are energetically more efficient and environmentally friendly since they eliminate hazardous fluids.²

Many solid refrigerant materials, especially magnetocaloric materials, have been investigated from experimental and theoretical viewpoints.³ The main drawbacks of solid refrigerant materials are associated with the hysteresis and high field change necessary to produce a considerable entropy change. The maximum entropy changes in usual magnetic materials are limited to the number of available magnetic states, given by the well known relation $\Delta S_T^{\text{max}} = R \ln(2J + 1)$. For example, in a simple Gd ($J = 7/2$) compound, we expect $\Delta S_T^{\text{max}} = 17.3 \text{ J mol}^{-1} \text{ K}^{-1}$. However, several giant magnetocaloric materials were reported and their ΔS_T -high values were ascribed to the coupling between magnetic and crystallographic phase transitions and deformations.⁴⁻⁶

The barocaloric effect was investigated in several works and materials, e.g., $\text{Pr}_x\text{La}_{1-x}\text{NiO}_3$ (Ref. 7) and ErCo_2 (Ref. 8), and the observed ΔS_T -values were lower compared with their respective limits $R \ln(2J + 1)$. Recently, Lloveras and coworkers⁹ reported giant barocaloric effects in ammonium sulphate $[(\text{NH}_4)_2\text{SO}_4]$ of about $\Delta S_T^{\text{max}} = 60 \text{ J K}^{-1} \text{ kg}^{-1}$ upon hydrostatic pressure variations $|P - P_{\text{am}}| \approx 1 \text{ kbar}$, leading to a refrigerant capacity of $\text{RC} = 276 \text{ J Kg}^{-1}$. More recently, Sandeman reported the high barocaloric potential in spin crossover materials from the thermodynamic point of view.¹⁰

In this work, we focus on the iron (II) system of octahedral symmetry where transition occurs from the diamagnetic

($S = 0$) low spin (LS) state (t_{2g}^6) to paramagnetic ($S = 2$) high spin (HS) state ($t_{2g}^4 e_g^2$). In this process, a low magnetic entropy change is expected, $R \ln(2S + 1) \approx 13.4 \text{ J mol}^{-1} \text{ K}^{-1}$. However, a huge entropy change ($\sim 80 \text{ J mol}^{-1} \text{ K}^{-1}$) can be triggered through the spin crossover transition process due to the activation of the vibrational (phonon) quantum states.^{11,12} In this work, the barocaloric potential was investigated through the Ising-like microscopic model¹³ with application to the one-dimensional spin crossover system $[\text{Fe}(\text{hyptrz})_3](4\text{-chlorophenylsulfonate})_2\text{H}_2\text{O}$. This is an unusual system which presents several desired properties: (1) a very sharp transition from the LS to the HS state and vice-versa, (2) high pressure influence on phase transition temperature ($dT_C/dP = 240 \text{ K(GPa)}^{-1}$), and (3) low applied hydrostatic pressure induces a parallel shift in the molar fraction curve- $\gamma_{\text{HS}}(T, P)$ from $T = 177 \text{ K}$ to above room temperature. Besides, low thermal hysteresis in this system is very important in order to reduce the energy losses in refrigeration cycles.^{14,15}

The spin crossover system can be described by the Ising-like model Hamiltonian, first introduced by Wajnflaz and Pick.¹⁶

$$H = -h \sum_i \sigma_i - \sum_{\langle ij \rangle} \tilde{J}_{ij} \sigma_i \sigma_j + \frac{1}{2K} \omega^2 - P\omega, \quad (1)$$

where σ_i denotes the fictitious spin which operates on HS and LS states, leading to +1 and -1 eigenvalues, respectively. \tilde{J}_{ij} represents the intermolecular elastic interaction, coupling the (i) and (j)-molecules.¹⁷ $h = \frac{k_B T}{2} \ln(g_{\text{HS}}/g_{\text{LS}}) - \Delta(P)$, with $k_B T$ being the thermal energy; g_{HS} and g_{LS} account for the degeneracies of HS and LS states^{18,19} (for our calculation, we consider $\ln(g_{\text{HS}}/g_{\text{LS}}) = 6.9$ (Refs. 20 and 21); and $\Delta(P)$ is related to the crystalline electrical field energy gap between HS and LS states. This gap depends on the metal-ligand distance, and so, it is usually an increasing function of pressure.²² ω is the volumetric deformation

^{a)} Author to whom correspondence should be addressed. Electronic mail: von.ranke@uol.com.br

(assumed homogeneous and isotropic), K is the compressibility, and P is the applied hydrostatic pressure (our Hamiltonian is in pressure units, i.e., energy per volume).

In order to describe the pressure influence on crossover materials, two order parameters are defined, namely, ω and $\gamma_{HS} = (1 + \langle \sigma \rangle) / 2$ (the molar fraction of HS molecules; $\langle \dots \rangle$ indicates the thermal average). The coupling between the order parameters is taken into account, considering the elastic interaction in the first order term of the Taylor series,

$$\gamma_{HS}(T, P) = \frac{1}{2} \left[1 + \tanh \left(\frac{2(2\gamma_{HS} - 1)(J_0 + J_1\omega) + (k_B T / 2) \ln(g_{HS} / g_{LS}) - \Delta(P)}{k_B T} \right) \right], \quad (2)$$

$$S(T, P) = R \left[\ln(2 \cosh(x)) + \left[\frac{\ln(g_{HS} / g_{LS})}{2} - x \right] \times (2\gamma_{HS} - 1) + \frac{\ln(g_{HS} \cdot g_{LS})}{2} \right], \quad (3)$$

where R is the gas constant (the entropy was multiplied by the Avogadro number), x is the same argument introduced into the *hyperbolic tangent* function in relation 2, and $\omega = K[P + J_1(2\gamma_{HS} - 1)^2] / 2$ was obtained minimizing the Gibbs free energy. The $\langle \sigma \rangle^2$ -dependence of the deformation can lead to a first order phase transition in the γ_{HS} -order parameter.²³ The relations (2) and (3) can be used to calculate the barocaloric potential $\Delta S_T = S(T, P_2) - S(T, P_1)$ in crossover materials, upon a pressure change $\Delta P = P_2 - P_1$ in an isothermal process.

Figure 1 shows the temperature dependence of γ_{HS} in the one-dimensional polymeric spin crossover system $[\text{Fe}(\text{hyptrz})_3(4\text{-chlorophenylsulfonate})_2\text{H}_2\text{O}]$ at different pressures: $P = 1.0$ bar, 4.1 kbar, and 5.0 kbar. The symbols represent the experimental data,^{14,15} and the solid curves represent our simulations for *increasing temperature*. The calculation was performed using the adjusted model parameters: $K = 10^{-3} (\text{kbar})^{-1}$, $J_0 = 92$ kbar, and $J_1 = 260$ kbar (for a scaling

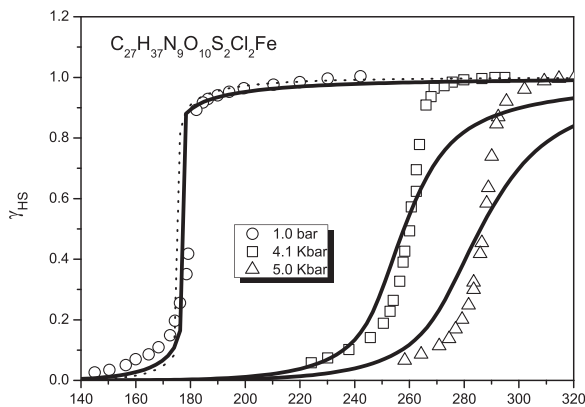


FIG. 1. Temperature dependence of the molar fraction γ_{HS} in $[\text{Fe}(\text{hyptrz})_3(4\text{-chlorophenylsulfonate})_2\text{H}_2\text{O}]$ upon different applied pressures. The symbols represent the experimental data and solid curves represent our simulations for *increasing temperature*. The dotted curve was calculated for *decreasing temperature*.

i.e., $\tilde{J} = J_0 + J_1\omega$. For a linear (1D) Ising model, an exact solution can be obtained for γ_{HS} Ref. 12. However, in order to obtain expressions to describe (1D), (2D), and (3D) spin-crossover systems (without losing the general thermodynamic behavior of the linear system), we considered the Hamiltonian in molecular field approximation (MFA).²¹ In MFA, embodying the number of first neighbors in the \tilde{J} parameter, the γ_{HS} state equation and the entropy are given by the following relations:

volume factor 0.14 \AA^3 , these values are similar to those reported by Gudyma *et al.*²¹). The energy gap was adjusted for each pressure $\Delta = 609$ kbar ($P = 1.0$ bar), 891 kbar ($P = 4.1$ kbar), and 988 kbar ($P = 5.0$ kbar). The high variation of Δ , which is related to the crystal field, is supported in spin-crossover materials due to a large variation (up to about 10%), e.g., in the Fe-N bond length.²⁴ The pressure stabilizes the LS phase state since the decrease in the distance between Fe-N bond (increasing Δ) and the electron-electron repulsion (which favor the HS phase), being an intra-atomic quantity, is rather insensitive to the lattice deformation. For $P = 1$ bar, γ_{HS} vs. T curve shows a discontinuity around $T = 178$ K, indicating a first order phase transition process. The thermal hysteresis width of 4 K was calculated (see the dotted curve in Fig. 1, simulated upon *decreasing temperature*), and it is in good agreement with the measured experimental data, namely, 5 K, as discussed in Ref. 14. For $P = 4.1$ and 5.0 kbar, no thermal hysteresis is predicted in accordance with the experimental measurements at these pressures. However, the hysteresis width shows a non-monotonic character, i.e., it reappears above 5 kbar as experimentally reported in Ref. 14.

Figure 2 shows the temperature dependence of the entropy changes in isothermal processes upon applied pressure changes from $P = 1.0$ bar to 4.1 and 5.0 kbar and from $P = 4.1$ to 5.0 kbar (solid curves). The open circles²⁵ represent the barocaloric potential in $\text{Gd}_5\text{Si}_2\text{Ge}_2$ for applied hydrostatic pressure changes from 1 bar to 2.9 kbar, and the full circles represent the magnetocaloric potential in $\text{Gd}_5[\text{Si}_{0.43}\text{Ge}_{0.57}]_4$ for the applied magnetic field variation from zero to 5 T, Ref. 26. It should be highlighted that these Gd-Si-Ge systems are the examples of giant induced caloric effect materials due to the almost simultaneous magnetic and crystallographic phase transitions.²⁷ The squares represent some experimental data of the giant barocaloric material $[(\text{NH}_4)_2\text{SO}_4]$ upon a pressure change $|P - P_{\text{atm}}| \approx 1$ kbar, from Ref. 9. Our results show huge ΔS_T -values around $55.8 \text{ Jmol}^{-1}\text{K}^{-1}$ (or $66 \text{ JK}^{-1}\text{kg}^{-1}$ for our system $\text{C}_{27}\text{H}_{37}\text{N}_9\text{O}_{10}\text{S}_2\text{Cl}_2\text{Fe}$). The high ΔS_T -values are observed in a large temperature range as is desirable for the tuning refrigeration process in a wide temperature interval. Usual magnetic refrigerant compounds have low limited values for the maximum entropy change associated with the number of available magnetic states. In addition, considerable

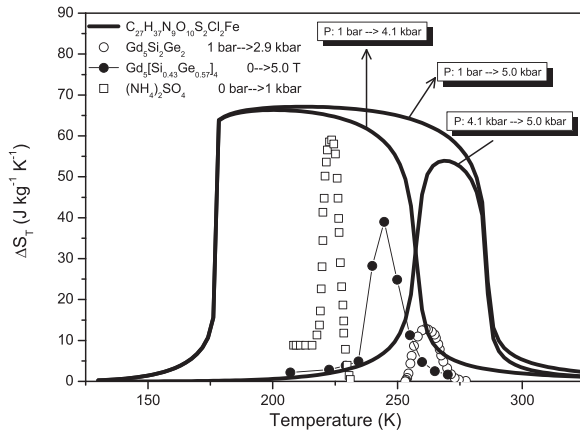


FIG. 2. Temperature dependence of isothermal ΔS_T calculated upon different pressure variations for the crossover material [Fe(hytrz)₃](4-chlorophenylsulfonate)₂H₂O (solid curves). For comparison, the giant barocaloric materials Gd₅Si₂Ge₂ (open circles) and [(NH₄)₂SO₄] (squares) and the giant magnetocaloric material Gd₅[Si_{0.43}Ge_{0.57}]₂ (full circles) were included.

ΔS_T -values are observed in a sharp temperature interval around the magnetic phase transition. In a spin-crossover material, due to the large number of available states, we can achieve $\Delta S_T^{\max} \approx 80 \text{ J mol}^{-1} \text{ K}^{-1}$ (which includes magnetic and phonon contributions).^{11,12} Besides, the critical temperature T_C ($\gamma_{HS}(T_C) = 1/2$) can be tuned with pressure in a wide temperature range (for $\Delta P : 1 \text{ bar} \rightarrow 4.1 \text{ kbar}$, we achieve $\Delta T \approx 80 \text{ K}$). The refrigerant capacity (RC) is calculated by integrating the ΔS_T curve over the temperature range at half maximum. For $\Delta P : 1 \text{ bar} \rightarrow 4.1 \text{ kbar}$, we obtain 2160 J mol^{-1} , which is about 6 times larger than the value of 350 J mol^{-1} , reported for the giant caloric material Gd₅Si₂Ge_{1.9}Fe_{0.1} (upon applied magnetic field variations from zero to 5 T).²⁸

Next, we will describe the microscopic cooling process mechanism. For simplicity, the spin-crossover system with iron-II is represented by a FeN₆ core where Fe is centered in an octahedron upon the influence of an isotropic harmonic potential, as displayed in Figure 3. The harmonic potentials in HS and LS states are represented by parabolas $U(R) = \frac{m_S}{2} \omega_S^2 (R - R_S)^2 + U_0^S$, where m_S , ω_S , and U_0^S are the Fe-mass, frequency, and minimum potential in $S=HS$ and LS states. The Fe ion in the two spin states has different vibrational frequencies ($\omega_{LS} > \omega_{HS}$) and Fe-N distances

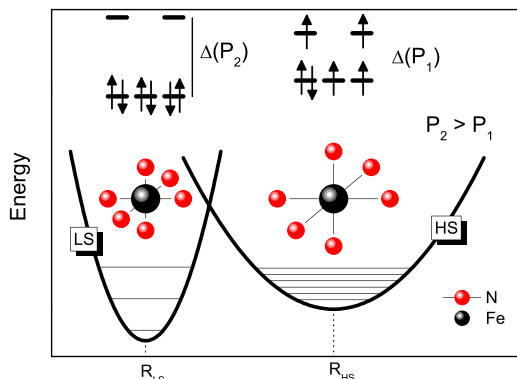


FIG. 3. Schematic representation of the electronic configurations and potential wells of Fe (II) (in FeN₆ octahedron) changes from the HS to the LS state upon pressure variations from $P_1 \rightarrow P_2$ ($P_2 > P_1$).

($R_{LS} < R_{HS}$). From quantum mechanics, the energetic distance between consecutive harmonic oscillator states is given by $\Delta \epsilon_S = \hbar \omega_S$, leading to $\Delta \epsilon_{LS} > \Delta \epsilon_{HS}$. In addition, each vibrational excited energy level $\epsilon_n = (n + 3/2)\hbar \omega_S$ is degenerate, and the degeneracy $g_S^{\text{phon}} = (n + 1)(n + 2)/2$ increases fast with energy. In this way, the HS and LS states present different values of vibration degeneracy ($g_{HS}^{\text{phon}} > g_{LS}^{\text{phon}}$), typically ($g_{HS}^{\text{phon}}/g_{LS}^{\text{phon}} \sim 1000$).²⁰ Besides different vibrational configurations, the HS and LS states present different spin states, namely, $t_{2g}^4 e_g^2$ ($S=2$) and t_{2g}^6 ($S=0$) for HS and LS states, respectively, as shown in Figure 3. Upon hydrostatic pressure variations from P_1 to P_2 ($P_2 > P_1$), an induced HS \rightarrow LS phase transition (spin crossover) occurs (Fig. 3). The pressure decreases the Fe-N distance, increasing the crystalline electrical field interaction $\Delta(P_2) > \Delta(P_1)$, which overcomes the pairing energy, leading to the LS configuration. Since the entropy is strongly correlated with the accessible quantum states, a huge entropy change can be obtained due to the LS \rightarrow HS and LS \rightarrow HS phase transitions, upon controlled pressure changes. The main contribution comes from different HS and LS-phonon spectra of energy, which is taken into account by the factor $\ln(g_{HS}/g_{LS})$, in our relation 3 (the spin and orbital degeneracies are also included in this factor).

Between two isobaric curves $S(T, P_1)$ and $S(T, P_2)$, a proper thermodynamic cycle can be considered for the refrigeration process, as fully discussed for magnetocaloric systems.²⁹ Investigations on spin-crossover materials may represent a major breakthrough in solid materials to be considered as refrigerant materials.

This work is dedicated to the memory of my colleague Karl A. Gschneidner, Jr.

This work was supported by CNPq—Conselho Nacional de Desenvolvimento Científico e Tecnológico.

- ¹P. J. von Ranke, S. Gama, A. Magnus, G. Carvalho, P. O. Ribeiro, B. P. Alho, T. S. T. Alvarenga, E. P. Nobrega, A. Caldas, V. S. R. de Sousa, P. H. O. Lopes, and N. A. de Oliveira, *J. Appl. Phys.* **118**, 243901 (2015).
- ²K. A. Gschneidner, Jr. and V. K. Pecharsky, *Int. J. Refrig.* **31**, 945 (2008).
- ³N. A. de Oliveira and P. J. von Ranke, *Phys. Rep.* **489**, 89 (2010).
- ⁴V. K. Pecharsky and K. A. Gschneidner, Jr., *Phys. Rev. Lett.* **78**, 4494 (1997).
- ⁵F. Hu, B. Shen, J. Sun, and Z. Cheng, *Appl. Phys. Lett.* **78**, 3675 (2001).
- ⁶H. Wada and Y. Tanabe, *Appl. Phys. Lett.* **79**, 3302 (2001).
- ⁷K. A. Müller, F. Fauth, S. Fischer, M. Koch, A. Furrer, and P. Lacorre, *Appl. Phys. Lett.* **73**, 1056 (1998).
- ⁸N. A. de Oliveira, *Appl. Phys. Lett.* **90**, 052501 (2007).
- ⁹P. Lloveras, E. Stern-Taulats, M. Barrio, J.-L. I. Tamarit, S. Crossley, W. Li, V. Pomjakushin, A. Planes, L. I. Moñosa, N. D. Mathur, and X. Moya, *Nat. Commun.* **6**, 8801 (2015).
- ¹⁰K. G. Sandeman, *APL Mater.* **4**, 111102 (2016).
- ¹¹E. König, G. Ritter, and S. K. Kulshreshtha, *Chem. Rev.* **85**, 219 (1985).
- ¹²M. Sorai and S. Seki, *J. Phys. Chem. Solids* **35**, 555 (1974).
- ¹³S. Klokishner, J. Linares, and F. Varret, *Chem. Phys.* **255**, 317 (2000).
- ¹⁴Y. Garcia, V. Ksenofontov, G. Levchenko, and P. Gülich, *J. Mater. Chem.* **10**, 2274 (2000).
- ¹⁵P. Gülich, V. Ksenofontov, and A. B. Gaspar, *Coord. Chem. Rev.* **249**, 1811 (2005).
- ¹⁶J. Wajnzilaz and R. Pick, *J. Phys. (Paris), Colloq.* **32**, C1 (1971).
- ¹⁷A. Gîndulescu, A. Rotaru, J. Linares, M. Diminian, and J. Nasser, *J. Phys.: Conf. Ser.* **268**, 012007 (2011).
- ¹⁸J. Wajnzilaz, *Phys. Status Solidi* **40**, 537 (1970).
- ¹⁹R. Zimmermann and E. König, *J. Phys. Chem. Solids* **38**, 779 (1977).
- ²⁰J. A. Nasser, K. Boukhebbaden, and J. Linares, *Eur. Phys. J. B* **39**, 219 (2004).

- ²¹I. Gudyma, V. Ivashko, and J. Linares, *J. Appl. Phys.* **116**, 173509 (2014).
- ²²J. Jeffic, H. Romsted, and A. Hauser, *J. Phys Chem. Solids* **57**, 1743 (1996).
- ²³C. P. Bean and D. S. Rodbell, *Phys. Rev.* **126**, 104 (1962).
- ²⁴L. Wiehl, G. Kiel, C. P. Köhler, H. Spiering, and P. Gütlich, *Inorg. Chem.* **25**, 1565 (1986).
- ²⁵S. Yuce, M. Barrio, B. Emre, E. S. Taulats, A. Planes, J. L. Tamarit, Y. Mudryk, K. A. Gschneidner, Jr., V. K. Pecharky, and L. Mañosa, *Appl. Phys. Lett.* **101**, 071906 (2012).
- ²⁶K. A. Gschneidner, Jr. and V. K. Pecharsky, *J. Appl. Phys.* **85**, 5365 (1999).
- ²⁷P. J. von Ranke, N. A. de Oliveira, and S. Gama, *J. Magn. Magn. Matter* **277**, 78 (2004).
- ²⁸R. Caballero-Flores, V. Franco, and A. Conde, *Appl. Phys. Lett.* **96**, 182506 (2010).
- ²⁹P. J. von Ranke, D. F. Grangeia, A. Caldas, and N. A. de Oliveira, *J. Appl. Phys.* **93**, 4055 (2003).